

Conformational Change and Orientation Fluctuations Prior to the Crystallization of Syndiotactic Polystyrene

Go Matsuba,[†] Keisuke Kaji,^{*,†} Koji Nishida,[†] Toshiji Kanaya,[†] and Masayuki Imai[‡]

Institute for Chemical Research, Kyoto University, Uji, Kyoto-fu 611-0011, Japan, and Department of Physics, Faculty of Science, Ochanomizu University, Otsuka, Bunkyo-ku, Tokyo 112-0012, Japan

Received April 26, 1999; Revised Manuscript Received October 19, 1999

ABSTRACT: Aiming to clarify the mechanism of crystal nucleation of polymers, we have made a quantitative investigation about the conformational change of syndiotactic polystyrene (sPS) during the induction period (ca. 30 min) when crystallized at 120 °C, 25 K above the glass transition temperature $T_g = 95$ °C, from the glassy state, i.e., for the so-called glass crystallization by time-resolved Fourier transform infrared (FT-IR) spectroscopy. It was found that even in the induction period, the absorbance of trans conformation bands begins to increase and it continues to increase not only through the induction period but also after crystallization. This suggests that the length of rodlike segments consisting of trans sequences starts to increase in the induction period. In this connection, Doi's theory on the isotropic-to-nematic transition of polymer liquid crystals has predicted that the extension of these segments triggers the orientation fluctuations of the rod segments because the increase of their excluded volumes makes the system unstable. To confirm such orientation fluctuations directly, we have also carried out time-resolved depolarized-light-scattering (DPLS) measurements. With the temperature jump to 120 °C from the glass, orientation fluctuations actually begin to occur and increase exponentially with time in the induction period. These results also support a previous proposal that a spinodal-decomposition-type microphase separation due to orientation fluctuations occurs in the induction period.

Introduction

A great number of studies on polymer crystallization have been reported,^{1–6} but most of them have been done mainly focusing on the crystal nucleation and growth; the structural formation during the induction period before crystal nucleation has hardly been studied. What happens in such preparatory processes is one of the most important unsolved problems in polymer physics. In this connection, an experimental finding has recently drawn attention that a small-angle X-ray scattering (SAXS) peak, the so-called long period peak, emerges before crystalline wide-angle X-ray scattering (WAXS) peaks. This was first discovered in the case of crystallization from oriented melts by Katayama and co-workers,^{7,8} i.e., the crystallization during melt spinning process,⁷ and from the stretched state of cross-linked melt,⁸ and subsequently it was reconfirmed in the crystallization from the oriented glassy state by Strobl and co-workers,^{9,10} Cakmak and co-workers¹¹ and Ryan and co-workers¹² confirmed it from the on-time SAXS and WAXS studies on melt-spinning and extrusion, respectively, using synchrotron radiation. Further, Ryan and co-workers¹² showed that such a phenomenon occurs even in the case of crystallization from quiescent melts. Although this finding is important to understand the polymer crystallization, we discovered a much more important phenomenon that a new peak, different from the long period peak, appears at lower q in SAXS from the very beginning of the induction period and grows with time.¹³

For the last 10 years, we have been studying this completely new phenomenon using poly(ethylene terephthalate) (PET) by SAXS,^{13,14} small-angle neutron scat-

tering (SANS),^{15,16} and depolarized light scattering (DPLS)^{15,17} techniques. Surprisingly, the SAXS studies^{13,14} revealed that the newly discovered SAXS peak is due to spinodal decomposition (SD). Probably a similar result was also obtained for poly(ether ketone) (PEKK) by Ezquerro et al.¹⁸ Although the long period peak appearing before crystallization is as well discussed in terms of SD, it should be noted that these two SD's are completely different. The first SD occurs due to orientation fluctuations in the whole system, and the second SD, giving the long period, may occur in the ordered domains formed in the first SD. Hence, the characteristic wavelength of the first SD is always larger than that of the second SD, and furthermore, the former largely depends on crystallization temperature¹⁹ but the latter does not change so much with crystallization temperature. The DPLS studies^{15,17} showed that orientation fluctuations or partial parallel ordering of polymer rigid segments actually occur during the induction period of crystallization which could be understood in analogy with the isotropic-to-nematic transition of liquid crystals. Using a novel technique of magnetic orientation, Kimura et al.²⁰ also confirmed that such orientation fluctuations do occur prior to crystallization. Moreover, Fukao and Miyamoto²¹ found the existence of a dynamical transition of amorphous phase from the so-called α process to another relaxation process, called the α' process, prior to crystallization.

According to a theory by Doi et al.,^{22–25} the isotropic-to-nematic transition, i.e., the parallel ordering of rod molecules, is triggered by extension of the rods when their length exceeds a critical value. In fact, it was confirmed from the SANS measurements of a deuterium-labeled sample of PET^{16,17} that the rigid segments slightly extend in the very early stage of induction period to such an extent that their length exceeds a critical value for parallel ordering. A completely new

* To whom correspondence should be addressed. Telephone: +81-(0)774-38-3140. Fax: +81-(0)774-38-3146.

[†] Institute for Chemical Research.

[‡] Ochanomizu University.

approach for the SD in polymer crystallization was made by Olmsted et al.,²⁶ which we think is a promising theory for the first SD. They pointed out an important role of the conformational free energy of polymer chains, which does not contradict with the Doi's theory and is essential to understand our experimental results.

This study aims at confirming whether such conformational change and orientation fluctuations in the induction period are actually observed. For this purpose, time-resolved FT-IR and DPLS measurements in the induction period have been performed on syndiotactic polystyrene (sPS) when it is crystallized by jumping the temperature to 120 °C, 25 K above the glass transition temperature $T_g = 95$ °C, from the melt-quenched glassy state. To follow the conformational change by FT-IR measurements, it is absolutely necessary that the IR bands concerning the chain conformations must be well characterized. Fortunately, the IR bands of sPS have well been assigned by Kobayashi et al.^{27,28} The results will be discussed based on the theory by Doi et al.^{22–25} for the isotropic-to-nematic transition of liquid polymer crystals.

Experimental Section

Sample and Characterization. The sample which was kindly supplied from Idemitsu Petrochemical Co. Ltd. was a syndiotactic polystyrene (sPS) with a number-average molecular weight, $M_n = 2.93 \times 10^5$ and a polydispersity, $M_w/M_n = 2.08$. The syndiotacticity measured by ¹³C NMR is more than 96% racemic pentad configuration. An amorphous thin film 50 μm thick was obtained by quenching the molten sPS into ice–water after pressing at high temperature of 330 °C for 5 min to remove the memory of the original samples; the memory effect is reported to remain even when sPS sample was melted for 3 min at 320 °C.²⁹ Such a high-temperature treatment might cause the polymer to degrade, but the sample neither colored nor showed appreciable abnormal IR peaks due to degradation. The melting temperature T_m and glass transition temperature T_g of this sample were determined to be 270 and 95 °C, respectively, at a rate of increasing temperature 5 °C/min by differential scanning calorimetry (DSC) with Perkin-Elmer DSC 7. The former was obtained from the peak temperature in a DSC melting curve, which agrees well with a reported T_m value.³⁰ The degree of crystallinity, x_c , of this sample after annealing at 120 °C for 10 h was roughly estimated by a WAXS method because sPS hardly changes in density by crystallization;³¹ the specimen densities of this samples measured by a flotation method were almost constant at 1.043 g/cm³ independent of annealing time even after crystallization. Hence, we cannot estimate x_c from the density. The X-ray crystallinity was measured using a Rigaku Denki Rint 2200 diffractometer with Cu Kα by Hermans-Weidinger's method,³² which is very practical, and the basic equation is $x_c = I_c/(I_c + KI_a)$ where I_c and I_a are integrated intensities in a proper q region including the main diffraction peaks and $K = I_{100c}/I_{100a}$ is a constant of the order of unity, I_{100c} and I_{100a} corresponding to a completely crystalline and a completely amorphous specimen, respectively. Here K was assumed to be unity since it is unknown for sPS. The observed WAXS patterns of the amorphous and annealed specimens after correction for the background scattering were scaled so that the intensities at a reflection angle $2\theta = 17.2^\circ$ would agree with each other. The obtained value of x_c is about 29%, which is almost equal to the value reported by de Candia et al.³³

FT-IR Measurements. The time-resolved FT-IR measurements were performed on melt-quenched specimens under an isothermal annealing condition at 120 °C in a homemade temperature-controlled cell, using a Nicolet Impact 410 system at 3 min intervals.

DPLS Measurements. The time-resolved DPLS measurements were also carried out under the same annealing condition at 120 °C. A specimen on the hot stage was irradiated

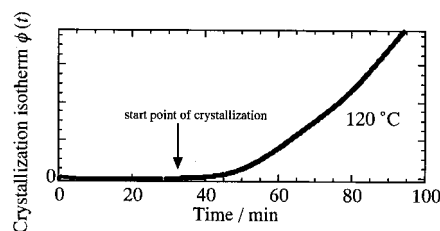


Figure 1. Annealing time dependence of crystallization isotherm at 120 °C for sPS after the temperature jump from the glassy state.

by a plane-polarized He–Ne laser beam ($\lambda = 632.8$ nm), and the scattered-light intensity under depolarized conditions was recorded by a photodiode array system at 0.5 min intervals. According to Stein et al.,³⁴ in the case of solids with randomly correlated orientation fluctuations, the Rayleigh factor $R_+(q)$ for crossed polaroids can be expressed by

$$R_+(q) = \left(\frac{\omega}{c}\right)^4 \frac{\langle \delta^2 \rangle}{15} \int_0^\infty g(r) \frac{\sin(qr)}{qr} 4\pi r^2 dr \quad (1)$$

where ω is the angular frequency of incident radiation, c is the velocity of light, $\langle \delta^2 \rangle$ is the mean-square anisotropy, and $g(r)$ is the function of orientation defined as $g(r) = (3 \langle \cos^2 \phi_{ij} \rangle_r - 1)/2$, where ϕ_{ij} is the angle between the optical axes of the i th and j th elements. The invariant due to the orientation fluctuations I_{VH} is given by

$$I_{\text{VH}} = \int_0^\infty R_+(q) q^2 dq = \frac{2\pi^2}{15} \left(\frac{\omega}{c}\right)^4 \langle \delta^2 \rangle \quad (2)$$

These equations, (1) and (2), give us a basis for interpretations of the results on the depolarized-light-scattering measurements.

Experimentally, however, we cannot obtain the invariant defined by eq 2 directly because the usual measurements are limited within a q range depending on the resolution of the spectrometer used. This problem can be avoided by employing an "integrated intensity", which is obtained by integrating the intensities in a q -independent region. The reason for this is as follows. When there exist no correlations among oriented domains and their sizes R are small enough compared with the wavelength of light, the scattering intensity becomes independent of q for $Rq \ll 1$. The intensity of this q range gives a value approximately proportional to the prefactor of integration of eq 1 or to the invariant of eq 2 because the remaining damping part of the scattering intensity for $Rq > 1$ may be negligible in the induction period where no large scatterers such as spherulites are formed. As is presumed, the scattering intensity during the induction period is independent of q at least within the observed q range 2.0–5.0 μm^{−1}. To show a measure of orientation we could use the height of the q -independent intensity region, but as a more reliable value of orientation fluctuations, we employed the integrated intensity in the measured q range.

Results and Discussion

DSC Measurements. Figure 1 shows the crystallization isotherm $\phi(t)$ at 120 °C as a function of annealing time t for a quenched sPS film which was measured by DSC. During the first 30 min, neither exotherm nor endotherm is observed, indicating the so-called induction period. Note that we also confirmed from WAXS measurements that no Bragg peaks appear during the induction period though the measurements were made on several films quenched after annealing for given times.

Conformational Change from FT-IR Measurements. Figure 2 shows the IR spectra of sPS's, melt-quenched and crystallized at 120 °C for 400 min. We

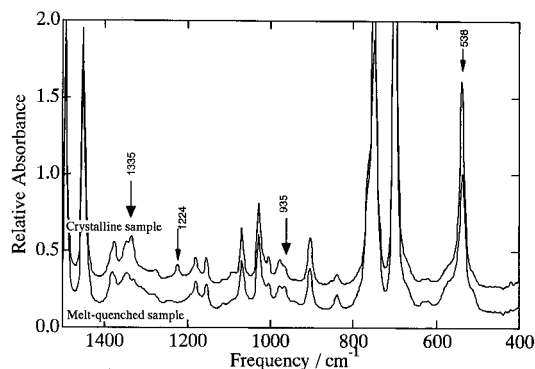


Figure 2. FT-IR spectra of crystalline (upper) and amorphous (lower) sPS samples in the region 400–1500 cm^{-1} . The bands marked by arrows appear after crystallization. The crystalline sample was annealed at 120 $^{\circ}\text{C}$ for 400 min.

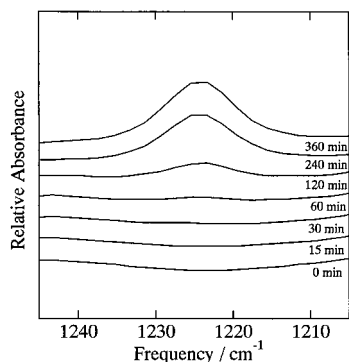


Figure 3. Change of the FT-IR spectrum of sPS in the region of 1200–1250 cm^{-1} when annealed at 120 $^{\circ}\text{C}$. The 1224 cm^{-1} band due to the crystalline chain packing for the α -crystal phase appears after 30 min, showing that the induction period of crystallization is 30 min.

can clearly see the appearance of new absorption bands at 1224 and 538 cm^{-1} for the crystallized sPS, showing that the crystal is in the α phase,^{28,35} with an all-trans conformation. According to Kobayashi et al.²⁸ the 1224 cm^{-1} band is caused by the packing of the chains in the crystalline state, but some bands around 538 cm^{-1} have been assigned to the conformational changes. In fact, Figure 3 shows that the 1224 cm^{-1} band does not change during the first 30 min after temperature jump to 120 $^{\circ}\text{C}$ while it begins to increase in intensity after the beginning of crystallization, suggesting again that the band at 1224 cm^{-1} originates from the chain packing in the crystalline state. The degree of crystallinity of the specimen annealed at 120 $^{\circ}\text{C}$ for 360 min seems to be less than 29% as indicated in the Experimental Section.

The absorption bands of sPS in the 500–600 cm^{-1} range have been assigned to out-of-plane modes of the phenyl group,²⁸ whose frequencies depend on the local skeletal conformations in the neighborhood of the phenyl group. Hence we need to examine the absorption bands in this range to know the change of chain conformations during the induction period. Figure 4 shows the time evolution of the enlarged spectrum in this range when the sample was annealed at 120 $^{\circ}\text{C}$. Here each curve is shifted along the axis of relative absorbance to make it easy to see. In the glassy state, three bands at 511, 537, and 572 cm^{-1} can be distinguished. Although the 548 cm^{-1} band is not apparent, it does seem to exist because otherwise we could not reasonably decompose the Lorentzian components. These bands are related to the skeletal conformations in terms

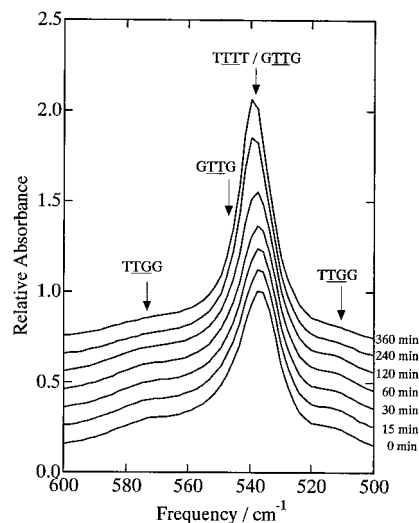


Figure 4. Change of the FT-IR spectrum of sPS in the region of 500–600 cm^{-1} when annealed at 120 $^{\circ}\text{C}$. The bands at 511, 537, 548, and 572 cm^{-1} are assigned to TTGG, TTTT/GTTG, GTTG, TTGG, respectively.

of tetrad sequences: 511 and 572 cm^{-1} are assigned to TTGG, 548 cm^{-1} to GTTG and 537 cm^{-1} to the mixture of GTTG and TTTT, respectively. Here T and G are trans and gauche, respectively, and the two middle italicized letters indicate the conformations around the C–C bonds on the both sides of the carbon atom bonded to a phenyl group. In the case of sPS, GTGT conformation could not be observed; its amount may be negligibly small.

If the polymer chain extends, it is expected that the TTTT band increases in intensity and the other bands including G conformation decrease because G conformation may convert to T conformation. This expectation can qualitatively be confirmed from Figure 4; the composite peak containing the TTTT band increases in intensity with annealing time while the peaks without this band decrease. Here it should be noted that the maximum position of the TTTT/GTTG composite band slightly shifts from 537 to 539.5 cm^{-1} with annealing time. This may be considered to be due to the conformational change of GTTG to TTTT. According to Kobayashi et al.,²⁷ the frequencies of GTTG and TTTT were evaluated to be 536 and 537 cm^{-1} on the basis of normal modes calculation. However, when the sample was annealed sufficiently, the peak position of the TTTT/GTTG band shifted to 539.5 cm^{-1} as seen from Figure 4. This suggests that the frequency of the pure TTTT is ca. 540 cm^{-1} . We do not know the exact value of the GTTG frequency, but if it is 536 cm^{-1} as cited above, the shift of the TTTT/GTTG band from 537 to 538 cm^{-1} would be elucidated qualitatively. With annealing, the GTTG conformation transforms to TTTT, and hence the intensity at 536 cm^{-1} decreases while that at 539.5 cm^{-1} increases; the former effect disappears, and the latter one is intensified. This causes the shift of the composite peak.

To make a quantitative analysis, we must decompose these bands. Especially the bands at 537 and 548 cm^{-1} overlap each other to make a single broad peak, and hence, the separation is essential. We decomposed the spectra in the region of 500–600 cm^{-1} into four components by assuming a Lorentzian shape for each band; Figure 5 indicates an example of such separation. The intensity of the band at 538 cm^{-1} (TTTT and GTTG)

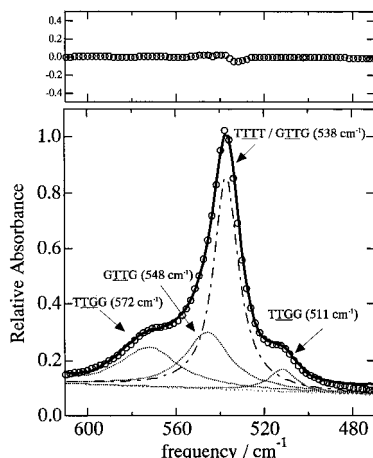


Figure 5. Separation of bands in the region 500–600 cm^{-1} of the FT-IR spectrum of sPS. An example for the amorphous quenched sample is shown.

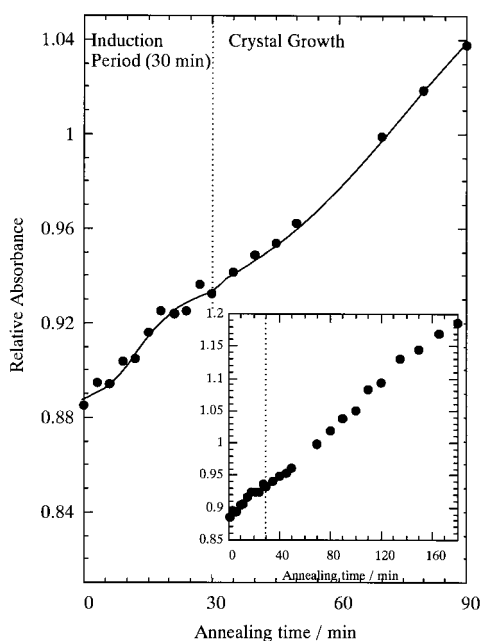


Figure 6. Annealing time dependence of the intensity of the 537 cm^{-1} band (TTTT/GTTG). The intensities are normalized to that immediately after temperature jump to 120 $^{\circ}\text{C}$.

after separation is plotted against annealing time in Figure 6, and those at 511 (TTGG), 548 (GTTG), and 572 cm^{-1} (TTGG) are plotted in Figure 7. The 538 cm^{-1} band including TTTT conformation starts to increase in intensity just after jumping to the crystallization condition and continues to increase not only through the induction period but also after crystallization begins, as shown in the inset of Figure 6. Correspondingly the bands at 511, 548, and 572 cm^{-1} , including gauche conformations, decrease in intensity with time in the induction period as well as during the crystallization stage (Figure 7). These results suggest that the TTGG and GTTG conformations change to the TTTT conformation even in the induction period. The increase of TTTT conformation may be considered to involve the expansion of a polymer chain, and the continuing increase of this band in the crystallization stage is very natural because the amorphous chains transform to the α -crystal phase with a trans-zigzag conformation in the crystallization process, accompanying the chain extension. For PET, such an extension of rigid segments in

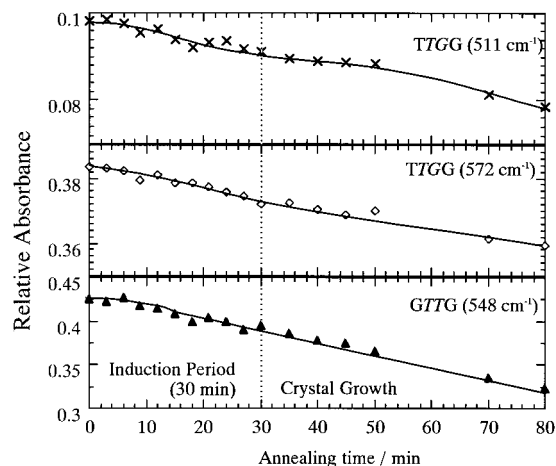


Figure 7. Annealing time dependence of the intensities of the 511 cm^{-1} (TTGG), 548 cm^{-1} (GTTG), and 572 cm^{-1} (TTGG) bands. The intensities were normalized to that immediately after temperature jump to 120 $^{\circ}\text{C}$.

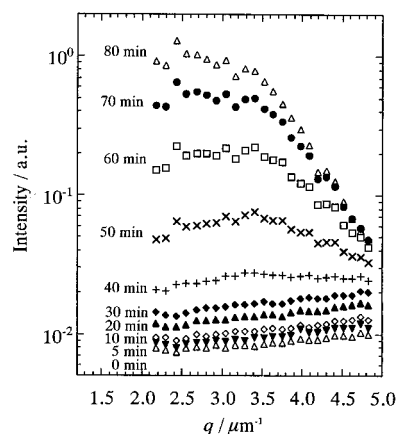


Figure 8. Depolarized light scattering profiles $I(q)$ of sPS films when annealed at 120 $^{\circ}\text{C}$ as a function of annealing time.

the induction period was directly observed from the SANS measurements of persistence length.^{15,16}

In the conclusion, the present results of time-resolved FT-IR measurements have confirmed that, even in the induction period, sPS chains actually extend by transforming their conformations from gauche to trans.

Orientation Fluctuations from DPLS Measurements. DPLS measurements were performed under the same annealing condition as that for the FT-IR measurements in order to confirm whether the orientation fluctuations actually evolve with time in the induction period. Figure 8 shows the semilogarithmic expression of time evolution of the DPLS intensity at 120 $^{\circ}\text{C}$ as a function of the length of scattering vector, q . There is no doubt that the depolarized light scattering intensity increases with annealing time even in the induction period, suggesting that the parallel ordering of polymer chains proceeds before crystal nucleation.

As seen in Figure 8, during the induction period of 30 min, the scattering profiles are almost independent of q , but the total intensity increases with annealing time. This fact indicates that the oriented domains are much smaller compared with the sizes corresponding to the measured q range. After the start of crystallization, the scattering profile becomes q -dependent; the intensity decreases with increasing q in the higher q

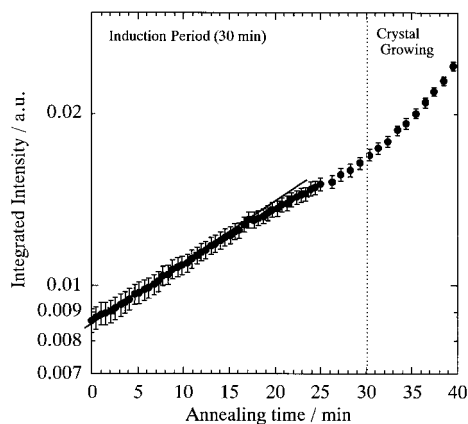


Figure 9. Annealing time dependence of the integrated intensity for the depolarized light scattering of sPS in the induction period of crystallization.

range. This means that the sizes of orientated domains of their aggregates become comparable with the q range.

Figure 9 shows the time dependence of the integrated intensity for orientation fluctuations, I_{VH} (eq 2), which was integrated within a measured q range of 2.0–5.0 μm^{-1} . In the early stage of the induction period, until about 17 min, the integrated intensity begins to increase with time while its amount is not large. This intensity growth is exponential, indicating a characteristic feature for the kinetics of spinodal decomposition in the isotropic-to-nematic transition of liquid crystal as shown by Doi et al.^{22–25} as was also shown in the case of PET crystallization.^{15,17} This again supports that in the induction period the parallel ordering of the rigid segments in the polymer actually proceeds. Hence, we can conclude that the increase of the length of rod segments immediately after temperature jump causes the parallel ordering of the rod segments themselves. After 17 min, the growth rate of the integrated intensity is slightly slowed, but it is beyond the experimental error. We may therefore separate the induction period into the early and late stages of the induction period as in the case of PET.^{15,17} When the crystallization starts, the integrated intensity naturally begins to increase more steeply again, which is considered to be caused by the growth of crystallites.

Doi et al. have theoretically investigated dynamics of formation of liquid crystalline phase in a stiff polymer system using a kinetics of two order parameters of concentration and orientation. This theory predicts that in the isotropic-to-nematic transition a spinodal decomposition type of phase separation occurs when the system is brought into a thermodynamically unstable region. This unstable state is caused by the increase of excluded volume due to the polymer chain extension. The critical concentration at which the isotropic phase becomes unstable is given by²²

$$\nu^* = \frac{4.19}{bL^2} \quad (3)$$

where b and L are the diameter and the length of the rodlike polymer and the excluded volume of this polymer is on the order of bL^2 . When the mean number of the rodlike polymers in the unit volume ν is smaller than ν^* , the system is stable and the orientation fluctuations cannot grow with time, but when $\nu > \nu^*$, the system becomes unstable and the orientation fluctuations start to grow. This theory also predicts that the dynamics of

isotropic-to-nematic transition is very similar to that of the spinodal-decomposition type phase separation. As shown above, we observed an exponential growth of the orientation fluctuations in the induction period (see Figure 9), which is one of the characteristic features of spinodal decomposition. In this case, we must examine whether the system fulfills the unstable condition ($\nu > \nu^*$) when the orientation fluctuations begin to occur.

The above theory has originally been formulated for solutions of stiff polymers. However, sPS is not a stiff polymer but a flexible one, and furthermore, the present system is not a solution but a bulk. Therefore, evaluation of the criterion for the isotropic-to-nematic transition should be modified. Thus, we may assume the hypothetical freely jointed chain model proposed by Flory.³⁶ In other words it is assumed that the chain consists of connected freely rotating stiff segments with the length being equal to the persistence length of the real chain. L is taken to be the average length of stiff segments in the real chain and ν can be calculated from eq 4,

$$\nu = \frac{\rho N_A}{(L/l_0)M_0} \quad (4)$$

where ρ is the bulk density of the polymer, l_0 and M_0 are the length and molecular weight of the monomer, respectively, and N_A is Avogadro's number. For the glassy state of sPS, the persistence length is obtained to be 1.88 nm from literature³⁷ and the density measured by a flotation method is 1.044 g/cm³. Furthermore, the diameter of the rod, b , is taken from the calculation of all-trans conformations³⁸ to be 1.11 nm. With these values, ν^* and ν are calculated to be 1.07 and 0.804 segments/nm³, respectively. Since $\nu < \nu^*$, the glassy state is stable and without involving chain extension orientation fluctuations would not grow even if the segmental motions were sufficient. In other words, this also means that the melt state is stable because the glass is its frozen state.

When the sample was annealed above T_g , the length of the rod segment or the persistence length is supposed to increase as already described in the discussion of the FT-IR results because the orientation fluctuations actually occurred as is clear from the DPLS results. These observations suggest that ν should become larger than ν^* above T_g . The rod length giving such a critical condition can be calculated from eqs 3 and 4 assuming $\nu = \nu^*$ and was obtained to be 2.51 nm, corresponding to 10 consecutive TT conformations (monomers) 10(TT). The increment of the rod length is 0.7 nm, which corresponds to 2.5 monomers; if the segments are extended by two or three monomers, then orientational ordering will initiate.

Conclusions

To elucidate the nucleation mechanism in the crystallization process, we performed time-resolved FT-IR and DPLS measurements on sPS during the induction period of crystallization from the glassy state. First, we found in the time-resolved FT-IR measurements that the increase of trans conformations occurs immediately after the temperature jump to over T_g , leading to expansion of the polymer chain. Furthermore, the time-resolved DPLS measurements revealed that the orientation fluctuations due to parallel ordering of polymer chains begin to increase in the induction period. These results suggest that a certain minimum length of rigid

segments is required for the parallel ordering of polymer chains. This critical length can tentatively be determined on the basis of Doi's theory, the isotropic-to-nematic transition of liquid crystalline polymers.

Acknowledgment. This study has been supported by NEDO International Joint Research Grant for the project "Fundamental Studies on Crystallization of Polymers" and by the Grant-in-Aid for Scientific Research on Priority Area "Cooperative Phenomena in Complex Liquids" from the Ministry of Education, Science, Culture, and Sports, Japan. The authors greatly appreciate these foundations. They also thank Idemitsu Petrochemical Co. Ltd. for supplying syndiotactic polystyrene samples.

References and Notes

- (1) Mandelkern, L. *Crystallization of Polymers*; McGraw-Hill: New York, 1964.
- (2) Hoffman, J. D.; Davis, G. T.; Lauritzen, J. I., Jr. The Rate of Crystallization of Linear Polymers with Chain Folding. In *Treatise on Solid State Chemistry*; Hannay, N. B., Ed.; Plenum: New York, 1976; Vol. 3.
- (3) Wunderlich, B. *Macromolecular Physics, Vol. 2 (Crystal Nucleation, Growth, Annealing)*; Academic Press: New York, 1996.
- (4) Bassett, D. C. *Principles of Polymer Morphology*; Cambridge: London, 1981.
- (5) Sedláček, B., Ed. *Morphology of Polymer*; Walter de Gruyter: Berlin, 1986.
- (6) Dosiére, M., Ed. *Crystallization of Polymers*; Kluwer Academic: Dordrecht, The Netherlands, 1953.
- (7) Katayama, K.; Amano, T.; Nakamura, K. *Kolloid-Z. Z. Polym.* **1968**, *126*, 125–134.
- (8) Nogami, K. Morphology of Flow-Induced Crystallization of Polymers. Dissertation, Kyoto University, 1983.
- (9) Strobl, G. R. *The Physics of Polymers*; Springer-Verlag: Berlin, 1996.
- (10) Strobl, G. R. In *Trends in Non-Crystalline Solids*; Conde, A., Conde, C. F., Millán, M., Eds.; World Scientific: Singapore, 1992; pp 37–55.
- (11) Cakmak, M.; Teitge, A.; Zachmann, H. G.; White, J. L. *J. Polym. Sci., Part B: Polym. Phys.* **1993**, *31*, 371–381.
- (12) Terrill, N. J.; Fairclough, P. A.; Town-Andrews, E.; Komanschek, B. U.; Young, R. J.; Ryan, A. J. *Polymer* **1998**, *39*, 2381–2385.
- (13) Imai, M.; Mori, K.; Mizukami, T.; Kaji, K.; Kanaya, T. *Polymer* **1992**, *33*, 4451–4456.
- (14) Imai, M.; Mori, K.; Mizukami, T.; Kaji, K.; Kanaya, T. *Polymer* **1992**, *33*, 4457–4462.
- (15) Imai, M.; Kaji, K.; Kanaya, T.; Sakai, Y. *Phys. Rev. B* **1995**, *B52*, 12696–12704.
- (16) Imai, M.; Kaji, K.; Kanaya, T.; Sakai, Y. *Physica B* **1995**, *213&214*, 718–720.
- (17) Imai, M.; Kaji, K.; Kanaya, T. *Phys. Rev. Lett.* **1992**, *71*, 4162–4165.
- (18) Ezquerro, T. A.; López-Cabarcos, E.; Hsiao, B. S.; Baltà-Callaeja, F. J. *Phys. Rev. E* **1996**, *54*, 989.
- (19) Kaji, K.; Imai, M. Dynamics of Structure Formation during the Induction Period of Polymer Crystallization. In *The Physics of Complex Liquids*; Yonezawa, F., Tsuji, K., Kaji, K., Doi, M., Fujiwara, T., Eds.; World Scientific: Singapore, 1998.
- (20) Kimura, T.; Ezure, H.; Tanaka, S.; Ito, E. *J. Polym. Sci., B* **1998**, *36*, 1227–1233.
- (21) Fukao, K.; Miyamoto, Y. *Phys. Rev. Lett.* **1997**, *79*, 4613–4616.
- (22) Doi, M.; Edwards, S. F. *The Theory of Polymer Dynamics*; Clarendon Press: Oxford, England, 1986; Chapter 10.
- (23) Shimada, T.; Doi, M.; Okano, K. *J. Chem. Phys.* **1988**, *88*, 2815–2821.
- (24) Doi, M.; Shimada, T.; Okano, K. *J. Chem. Phys.* **1988**, *88*, 4070–4075.
- (25) Shimada, T.; Doi, M.; Okano, K. *J. Chem. Phys.* **1988**, *88*, 7181–7186.
- (26) Olmsted, P. D.; Poon, P. D.; McLeish, T. C. B.; Terrill, N. J.; Ryan, A. J. *Phys. Rev. Lett.* **1998**, *81*, 373–376.
- (27) Nakaoki, T.; Kobayashi, M. *J. Mol. Struct.* **1991**, *242*, 315–331.
- (28) Kobayashi, M.; Nakaoki, T.; Ishihara, N. *Macromolecules* **1989**, *22*, 4377–4382.
- (29) Guerra, G.; Vitagliano, V. M.; De Rosa, C.; Petraccone, V.; Corradini, P. *Macromolecules* **1990**, *23*, 1539–1544.
- (30) Zimba, C. G.; Rabolt, J. F.; English, A. D. *Macromolecules* **1989**, *22*, 2867–2869.
- (31) Kuramoto, M. *Polym. Prepr. Jpn.* **1994**, *43*, 77–80.
- (32) Alexander, L. E. *X-ray Diffraction Method in Polymer Science*; J. Wiley: New York, 1969; Chapter 3.
- (33) De Candia, F.; Ruvolo Filho, A.; Vittoria, V. *Colloid Polym. Sci.* **1991**, *269*, 650–654.
- (34) Koberstein, J.; Russel, T. P.; Stein, R. S. *J. Polym. Sci., Polym. Phys. Ed.* **1979**, *17*, 1719.
- (35) Greis, O.; Xu, Y.; Asano, T.; Petermann, J. *Polymer* **1989**, *30*, 590–594.
- (36) Flory, P. J. *Statistical Mechanics of Chain Molecules*; Interscience: New York, 1969.
- (37) Yamakawa, H. *Annu. Rev. Phys. Chem.* **1984**, *35*, 23–47.
- (38) Einaga, Y.; Koyama, H.; Konishi, T.; Yamakawa, H. *Macromolecules* **1989**, *22*, 3419–3424.

MA990641I